



OPEN

# Coalescing Majorana edge modes in non-Hermitian $\mathcal{PT}$ -symmetric Kitaev chain

C. Li<sup>2</sup>, L. Jin<sup>1</sup> & Z. Song<sup>1</sup>✉

A single unit cell contains all the information about the bulk system, including the topological feature. The topological invariant can be extracted from a finite system, which consists of several unit cells under certain environment, such as a non-Hermitian external field. We present an exact solvable non-Hermitian finite-size Kitaev chain with  $\mathcal{PT}$ -symmetric chemical potentials at the symmetric point. The straightforward calculation shows that there are two kinds of Majorana edge modes in this model divided by  $\mathcal{PT}$  symmetry-broken and unbroken. The one appeared in the  $\mathcal{PT}$  symmetry-unbroken region can be seen as the finite-size projection of the conventional degenerate zero modes in a Hermitian infinite system with the open boundary condition. It indicates a possible variant of the bulk-edge correspondence: The number of Majorana edge modes in a finite non-Hermitian system can be the topological invariant to identify the topological phase of the corresponding bulk Hermitian system.

The discovery of topological matter which exhibits topological properties in the band structure has opened a growing research field<sup>1–5</sup>. A particularly important concept is the bulk-edge correspondence, which indicates that, a nontrivial topological invariant in the bulk indicates localized edge modes that only appear in the presence of the open boundary in the thermodynamic limit. In general, a bulk system is constructed by stacking a great many copies of a single original unit cell in an array. In this sense, a single unit cell contains all the information about the bulk system, including the topological feature. Then the topological invariant can be, in principle, extracted from a finite system, which consists of several unit cells under certain environment, such as a non-Hermitian external field<sup>6–8</sup>. In fact, the original bulk-edge correspondence is an example in this context: The open boundary can be technically regarded as one of the extreme cases of adding local impurity on the bulk, that breaks the translational symmetry. On the other hand, it has been shown that a finite system with imaginary ending potentials can share the common eigenstates with an infinite system<sup>9–11</sup>. It implies that a finite non-Hermitian system may retain some of characteristics, such as zero-energy modes of an infinite Hermitian system. An interesting question is whether there is a generalization of the bulk-edge correspondence to non-Hermitian systems which arises from the imaginary impurity.

In this work, we investigate a non-Hermitian finite-size Kitaev ring with parity-time ( $\mathcal{PT}$  symmetric chemical potentials. We demonstrate that the key to retrieve the Majorana zero mode from a small system is a pair of specific imaginary chemical potentials, under which the coalescing zero mode shares the identical pattern with that of the conventional zero mode in the thermodynamic limit. The coalescing zero mode in a finite-size non-Hermitian system can be directly obtained from the projection of the conventional degenerate zero modes in a Hermitian infinite system. Exact solution also shows the existence of Majorana edge modes, which emerge as a pair of  $\mathcal{PT}$  symmetry breaking states with imaginary eigenvalues. It indicates a variant of the bulk-edge correspondence: The number of Majorana edge modes in a finite-size non-Hermitian system can be the topological invariant to identify the topological phase of the corresponding bulk Hermitian system.

## Results

**Model hamiltonians.** We consider a one-dimensional Kitaev model with two impurities. The Hamiltonian of the tight-binding model takes the following form

<sup>1</sup>School of Physics, Nankai University, Tianjin, 300071, China. <sup>2</sup>Department of Physics, University of Hong Kong, Hong Kong, China. ✉e-mail: [songtc@nankai.edu.cn](mailto:songtc@nankai.edu.cn)

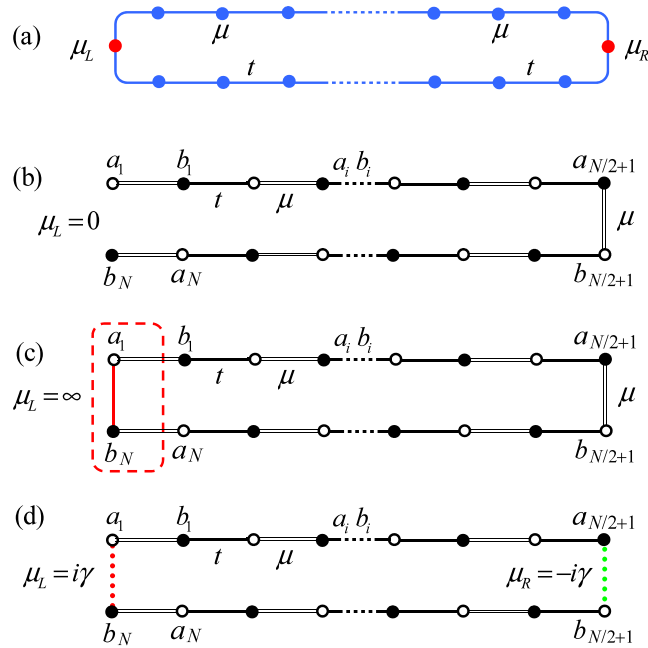


**Figure 1.** Schematic illustrations for edge modes in the Majorana Hamiltonian from Eq. (1), induced by impurities embedded in a Kitaev ring. **(a)**  $N$ -site Kitaev ring with uniform chemical potential  $\mu$  and hopping amplitude (pairing amplitude)  $N$ . Two impurities are located at sites 1 and  $N/2 + 1$ , in terms of specific values of chemical potentials  $\mu_L$  and  $\mu_R$ , respectively. The pairing term is omitted for the clarity. The corresponding Majorana lattice is a  $2N$ -site dimerized ring with staggered hopping strengths  $t$  (single line) and  $\mu$  (double line), which contains two specific dimers with hopping amplitudes  $\mu_L$  and  $\mu_R$ . We focus on three cases: **(b)**  $\mu_L = 0$ ,  $\mu_R = \mu$ , the lattice becomes a standard  $2N$ -site SSH chain, which possesses edge modes for  $\mu > 1$ . **(c)**  $\mu_L = \infty$ ,  $\mu_R = \mu$ , the dimer (circled by the dashed red line) is adiabatically eliminated, and then the lattice becomes a standard  $2(N - 1)$  SSH chain, which possesses edge modes for  $\mu < 1$ . For infinite  $N$ , the conclusions for cases **(b,c)** can be regarded as the extension of original bulk-edge correspondence. **(d)**  $\mu_L = -\mu_R = i\gamma$ , it is  $\mathcal{PT}$  symmetric. For finite  $N$ , it has two coalescing zero modes for  $\mu > 1$ , while two imaginary-energy modes for  $\mu < 1$  with two coalescing zero modes still exist. All these modes exhibit evanescent wave behavior. The number of edge modes for finite system matches the topological invariant of the bulk. It indicates that bulk-edge correspondence can be extended to the non-Hermitian regime.

$$\begin{aligned}
 H &= H_0 + H_{\text{im}}, \\
 H_0 &= -\sum_{j=1}^N (tc_j^\dagger c_{j+1} + \Delta c_j^\dagger c_{j+1}^\dagger + \text{H.c.}) - \mu \sum_{j=1}^N (1 - 2n_j), \\
 H_{\text{im}} &= (\mu - \mu_L)(1 - 2n_1) + (\mu - \mu_R)(1 - 2n_{N/2+1}),
 \end{aligned}
 \tag{1}$$

where  $j$  is the coordinate of lattice sites and  $c_j$  is the fermion annihilation operator at site  $j$ .  $H_0$  is employed to depict  $p$ -wave superconductors. The hopping between (pair operator of) neighboring sites is described by the hopping amplitude  $t$  (the real order parameter  $\Delta$ ). The last term in  $H_0$  gives the chemical potential (see Fig. 1a). Imposing the periodic boundary condition  $c_1 \equiv c_{N+1}$ , the Hamiltonian  $H_0$  can be exactly diagonalized and the topological invariant can be obtained in various parameter regions. It provides well-known example of systems with the bulk-edge correspondence when the open boundary condition is imposed. It turns out that a sufficient long chain has Majorana modes at its two ends<sup>12</sup>. A number of experimental realizations of  $p$ -wave superconductors have found evidence for such Majorana modes<sup>13–18</sup>, also the realizations of Majorana modes<sup>19–21</sup>. Term  $H_{\text{im}}$  represents two impurities on the two symmetrical sites. The impurities are described in terms of specific values of chemical potentials  $\mu_L$  and  $\mu_R$ . We note that taking  $\mu_L = 0$  or  $\pm\infty$ , and  $\mu_R = \mu$ , it corresponds to the open Majorana chains with different edges (see Fig. 1b,c). It is an alternative representation of bulk-boundary correspondence. In this context, the real value of  $\mu_{L,R}$  requires an infinite system or lead to a trivial situation. In this work, we consider imaginary value of  $\mu_{L,R}$ . The imaginary potentials has been realized by the optical lattice and coupled array<sup>22–24</sup> and the realization of the non-Hermitian Kitaev model in the spin model context has been detected too<sup>25,26</sup>. In contrast to previous studies based on Hermitian chains in the thermodynamic limit, we focus on the Kitaev model on a finite lattice system. This is motivated by the desire to get a clear physical picture of the edge mode through the investigation of a small system. We first study the present model from the description in terms of Majorana fermions. We will show that the evident indicator for phase diagram does not require infinite system.

**Majorana representation.** In the following, which is showed in Fig. 1d, the impurity is taken as  $\mathcal{PT}$  symmetric with  $\mu_L = i\gamma$  and  $\mu_R = -i\gamma$ . Note that the Hamiltonian  $H$  is not  $\mathcal{PT}$  symmetric unless  $\Delta$  is pure imaginary. The  $\mathcal{PT}$  symmetric  $H$  with the twisted (or open) boundary condition has been studied in<sup>27</sup>. Here the space-reflection operator, or the parity operator  $\mathcal{P}$  and the time-reversal operator  $\mathcal{T}$ , are defined as

$$\mathcal{P}c_l^\dagger\mathcal{P} = c_{N+1-l}^\dagger, \mathcal{T}i\mathcal{T} = -i. \tag{2}$$

Nevertheless, we will see that the core matrix in the Majorana fermion representation is  $\mathcal{PT}$  symmetric, which ensures the system is pseudo-Hermitian.

We introduce Majorana fermion operators

$$a_j = c_j^\dagger + c_j, b_j = -i(c_j^\dagger - c_j), \tag{3}$$

which satisfy the relations

$$\begin{aligned} \{a_j, a_{j'}\} &= 2\delta_{jj'}, \{b_j, b_{j'}\} = 2\delta_{jj'} \\ \{a_j, b_{j'}\} &= 0, a_j^2 = b_j^2 = 1. \end{aligned} \tag{4}$$

Then the Majorana representation of the Hamiltonian is

$$\begin{aligned} \mathcal{H} &= -\frac{i}{4}\sum_{j=1}^N [(t + \Delta)b_j a_{j+1} + (t - \Delta)b_{j+1} a_j] \\ &\quad - \frac{i}{2}\sum_{j=1, N/2+1}^N \mu a_j b_j + \text{H.c.} \\ &\quad + \frac{\gamma}{2}(a_1 b_1 - a_{N/2+1} b_{N/2+1} - \text{H.c.}). \end{aligned} \tag{5}$$

The diagonalization of  $H$  is directly related to a model of two coupled SSH chain, which was systematically studied in ref.<sup>28</sup>.

**Edge modes.** Majorana edge mode plays an important role in the characterization of the topological feature of matter, such as the bulk-edge correspondence. The Majorana particle is localized at two ends. Since the pattern of the zero mode is exponentially decaying, the bound Majorana particle must require infinite chain condition. Therefore the conventional zero mode cannot exist in a Hermitian system except for some trivial cases<sup>29,30</sup>. In this paper, we focus on a finite-size non-Hermitian system and we define the edge mode by the evanescent wave characterization.

We consider a Kitaev ring at the symmetric point  $\Delta = t$ . We write down the Hamiltonian as the form

$$\mathcal{H} = \psi^T h \psi, \tag{6}$$

in the basis  $\psi^T = (a_1, b_1, a_2, b_2, a_3, b_3, \dots, a_N, b_N)$ , where  $h$  represents a  $2N \times 2N$  matrix. Here matrix  $h$  is explicitly written as

$$\begin{aligned} h &= -\frac{i}{2}\left(\sum_{l=1}^N t|2l\rangle\langle 2l+1| + \sum_{l=1, N/2+1}^N \mu|2l-1\rangle\langle 2l| + \text{H.c.}\right) \\ &\quad + \frac{\gamma}{2}(|1\rangle\langle 2| - |N+1\rangle\langle N+2| - \text{H.c.}) \end{aligned} \tag{7}$$

where basis  $\{|j\rangle, j \in [1, 2N]\}$  is an orthonormal complete set,  $\langle j|j'\rangle = \delta_{jj'}$ . By taking the linear transformation

$$\begin{cases} |\sigma, 2l-1\rangle = \frac{e^{-i\pi/4}}{2}(|2l\rangle + i\sigma|2N+3-2l\rangle) \\ |\sigma, 2l\rangle = \frac{e^{i\pi/4}}{2}(|2l+1\rangle - i\sigma|2N+2-2l\rangle) \end{cases} \tag{8}$$

with  $l \in [1, N/2]$  and  $\sigma = \pm$ , we can express matrix  $h$  as  $h = h_+ + h_-$  with

$$[h_+, h_-] = 0, \tag{9}$$

where

$$\begin{aligned} h_\sigma &= t\sum_{l=1}^{N/2} |\sigma, 2l-1\rangle\langle \sigma, 2l| - \mu\sum_{j=1}^{N/2-1} |\sigma, 2l\rangle\langle \sigma, 2l+1| \\ &\quad + \text{H.c.} + \sigma i\gamma(|\sigma, 1\rangle\langle \sigma, 1| - |\sigma, N\rangle\langle \sigma, N|). \end{aligned} \tag{10}$$

Obviously,  $h_{\pm}$  describes two identical SSH chains with opposite imaginary ending potentials  $\pm i\gamma$ . It is a  $\mathcal{PT}$  symmetric system and has been studied in refs.<sup>31</sup> for  $\mu > t$  and the topological phase in the similar systems has been studied in refs.<sup>32</sup>. It is shown that there is a single zero mode in such a finite degree of non-Hermiticity at the exceptional point (EP).

Now we concentrate on a single non-Hermitian SSH chain with the Hamiltonian

$$h_{\text{SSH}} = \sum_{l=1}^{N/2} |2l-1\rangle\langle 2l| - \sum_{l=1}^{N/2-1} \mu |2l\rangle\langle 2l+1| + \text{H.c.} + i\gamma(|1\rangle\langle 1| - |N\rangle\langle N|), \tag{11}$$

where we take  $t=1$  and  $\mu=0$  for the sake of simplicity. Based on the commutation relation between  $h_{+}$  and  $h_{-}$ , we can use  $h_{\text{SSH}} (h_{\text{SSH}}^{\dagger})$  to study the properties of  $h_{+}$  ( $h_{-}$ ). But one should attention that it does not means  $h_{\text{SSH}} (h_{\text{SSH}}^{\dagger}) = h_{+}$  ( $h_{-}$ ). Here we redefine the space-reflection operator, or the parity operator  $\mathcal{P}$  in the space spanned by the complete set  $\{|l\rangle\}$ . The action  $\mathcal{P}$  on  $|l\rangle$  is given by the equality

$$\mathcal{P}|l\rangle = |N+1-l\rangle. \tag{12}$$

Then we have  $[h_{\text{SSH}}, \mathcal{PT}] = 0$ , which implies that  $h_{\text{SSH}}$  is pseudo-Hermitian<sup>33</sup>, i.e.,  $h_{\text{SSH}}$  has either real spectrum or its complex eigenvalues occur in complex conjugate pairs. On the transition from a pair of real levels to a complex conjugate pair, or EP, two levels coalesce to a single level. The key point of our approach is to link the zero-eigenvalue coalescing eigenvector to the conventional Majorana zero mode in the thermodynamic limit.

The Bethe ansatz wave function  $|\psi_k\rangle = \sum_{l=1}^N f_l^k |l\rangle$  has the form

$$f_l^k = \begin{cases} A_k e^{ikl} + B_k e^{-ikl}, & l = 2j - 1 \\ C_k e^{ikl} + D_k e^{-ikl}, & l = 2j \end{cases}, \tag{13}$$

where  $j = 1, 2, \dots, N/2$ . Following the derivation in the Method C, if we take the  $\mu_L = i\gamma$  and  $\mu_R = -i\gamma$ , the appearance of the zero mode requires

$$\gamma = \mu^{1-N/2}, \tag{14}$$

and based on the specific form above, there are three types of eigenvector  $|\psi_k\rangle$ , with the eigenvalue (see details in the Method A)

$$\varepsilon_k = \pm \sqrt{1 + \mu^2 - \mu(e^{2ik} + e^{-2ik})}. \tag{15}$$

In general, the EP varies as the system size changes. In the present model,  $\gamma = \mu^{1-N/2}$  is  $N$  dependent except when  $\mu = 1$ . It is reasonable that the system is always at the EP for any  $N$ . We note that in the case of  $\mu = 1$ , it reduces to a uniform chain with  $\gamma = 1$ , which was studied in ref.<sup>34</sup>. The solutions for  $\mu \neq 1$  is concluded as follows.

(i) Scattering vector with real eigenvalues: In this case,  $k$  is a real number, the eigenvalue is real. The energy gap has a lower bound

$$\Delta_{\text{Gap}} \geq 2|1 - \mu|, \tag{16}$$

which is crucial to protect the degenerate ground states of the original Kitaev model from decoherence.

(ii) Coalescing vector with zero eigenvalue: Here the wave vector is imaginary,  $k = \pm \frac{i}{2} \ln \mu$ . The eigenvector has the form

$$|\psi_{\text{zm}}\rangle = \Omega \sum_{j=1}^{N/2} (\mu^{1-j} |2j-1\rangle - i\mu^{j-N/2} |2j\rangle), \tag{17}$$

satisfying

$$h_{\text{SSH}} |\psi_{\text{zm}}\rangle = 0. \tag{18}$$

where  $\Omega = \mu^{N/2-1} \sqrt{(1 - \mu^2)/(2 - 2\mu^N)}$  is the Dirac normalizing constant. It is  $\mathcal{PT}$  symmetric and has a zero biorthogonal norm, indicating the coalescence of two levels. Actually, the zero-mode vector for  $h_{\text{SSH}}^{\dagger}$  can be constructed as

$$|\eta_{\text{zm}}\rangle = \Omega \sum_{j=1}^{N/2} (\mu^{1-j} |2j-1\rangle + i\mu^{j-N/2} |2j\rangle), \tag{19}$$

satisfying

$$h_{\text{SSH}}^{\dagger} |\eta_{\text{zm}}\rangle = 0. \tag{20}$$

On the other hand, it is easy to check

$\mu$	$n_1$	$n_{EP}$	$n_S$	Symmetry
$\mu > 1$	0	1	$N-2$	$\mathcal{PT}$ – unbroken
$\mu < 1$	2	1	$N-4$	$\mathcal{PT}$ – broken

**Table 1.** For  $N$ -site system,  $\gamma = \mu^{1-N/2}$ ,  $n_1$  is the number of imaginary levels,  $n_{EP}$  is the number of coalescing state,  $n_S$  is the number of real levels. We have  $n_1 + 2n_{EP} + n_S = N$ .

$$\langle \eta_{zm} | \psi_{zm} \rangle = 0, \quad (21)$$

and

$$|\eta_{zm}\rangle = i\mathcal{P}|\psi_{zm}\rangle \text{ or } |\eta_{zm}\rangle = (|\psi_{zm}\rangle)^*, \quad (22)$$

which indicate that the vector  $|\psi_{zm}\rangle$  has a zero biorthogonal norm and the relations between two conjugate vectors. Based on these facts we conclude that the zero-mode vector  $|\psi_{zm}\rangle$  is a coalescing vector for  $\mu \neq 1$ . The exact wave function of  $|\psi_{zm}\rangle$  clearly indicates that it is a superposition of two parts with nonzero amplitudes only located at even or odd sites, respectively. We will show that vectors  $|\eta_{zm}\rangle$  and  $|\psi_{zm}\rangle$  have a close relation to the standard zero modes of a Hermitian chain in the thermodynamic limit. Here, the real value of  $\mu_{L,R}$  can still lead to two zero modes, but they are two degenerate states and with only one phase exists, no matter

(iii) Evanescent wave vector with imaginary eigenvalue: The derivation in the Method A shows that this kind of state only appears at  $\mu < 1$ . In this case,  $k$  is still imaginary. Since matrix  $h_{SSH}$  is pseudo-Hermitian, this type of eigenvector always appears in pair. The wave vector approximately takes

$$k = \pm i \frac{N-1}{2} \ln \mu \quad (23)$$

in large  $N$  or small  $\mu$  and the wave function reads

$$|\psi_{IM}^\sigma\rangle \approx \frac{1}{2}[(1 + \sigma)|1\rangle + (1 - \sigma)|N\rangle], \quad (24)$$

satisfying

$$h_{SSH}|\psi_{IM}^\sigma\rangle = i\sigma|\varepsilon_{IM}||\psi_{IM}^\sigma\rangle. \quad (25)$$

with approximate eigenvalue

$$\varepsilon_{IM} \approx \pm i\mu^{1-N/2}, \quad (26)$$

We can see that the  $\mathcal{PT}$  symmetry is broken. Both the two vectors present evanescent wave and

$$|\psi_{IM}^\sigma\rangle = \mathcal{PT}|\psi_{IM}^{-\sigma}\rangle, \quad (27)$$

which indicates that  $|\psi_{IM}^\pm\rangle$  are symmetry breaking. We summarize the solutions in Table 1 and present the numerical calculation of energy-levels of Hamiltonian (11) and the fidelity  $\langle n_{IM}^- | \psi_{IM}^- \rangle$  and  $\langle n_{zm} | \psi_{zm} \rangle$  respectively in Fig. 2, which shows the effectiveness of our analytical solution.

We would like to point out that the real value of  $\mu_{L,R}$  can still produce two zero modes (or just two eigenstates with zero energy) once they satisfy one condition (showed in the Method), but they are two degenerate states and with only one phase exists, no matter  $\mu > 1$  or  $< 1$ . It leads to a trivial model without symmetry breaking and coalescing even if there are some connections between the finite zero modes and conventional zero modes of Kitaev model. As we mentioned before, there are also researches focus on the  $\mathcal{PT}$  symmetric  $H$  with the twisted (or open) boundary condition where the similar edge modes can be found<sup>27</sup>, but with totally different topological meaning according to their system conditions. For a more general quasi-1D Kitaev chain with  $p_x + ip_y$  superconducting pairing<sup>18</sup>, Majorana zero modes emerge in such an open system without fine-tuning as a result of charge-conjugation symmetry, and Majorana dark state (MDS) can appear too.

It is well known that the number of Majorana zero mode for an infinite Hermitian Kitaev chain with open boundary conditions can be a topological invariant, referred as the bulk-edge correspondence. Similarly, the result in Table 1 indicates the number of Majorana edge modes in a finite non-Hermitian system can also be the topological invariant to identify the topological phase of the corresponding bulk Hermitian system. In this situation, two Majorana edge modes appear as a pair of  $\mathcal{PT}$  symmetry breaking states with imaginary eigenvalues, this can be regarded as a variant of the bulk-edge correspondence in the complex regime. Recently, non-Hermitian SSH chains were experimentally realized by coupled dielectric microwave resonators<sup>35,36</sup> and photonic lattices<sup>37,38</sup>. In Method B, we provide exact solutions for a 6-site system to demonstrate our main idea, which can be a protocol for the experimental investigation. Before, many works showed the connection between the Majorana zero modes (edge modes) and the topological properties of the Kitaev model in general condition ( $\Delta \neq t$ ) with the numerical simulation<sup>39-41</sup>, which give the phase diagram and indicate the difficulty of exact solution. Here, we only consider the Kitaev ring on the symmetric point  $\Delta = t$ , this simple situation is good enough to give a clear physical picture and solution to show that how the appearance of non-zero  $\mu_R$  and  $\mu_L$  change the topology of the system and how the edge modes (zero modes) connects with conventional ones in a large  $N$  limit.

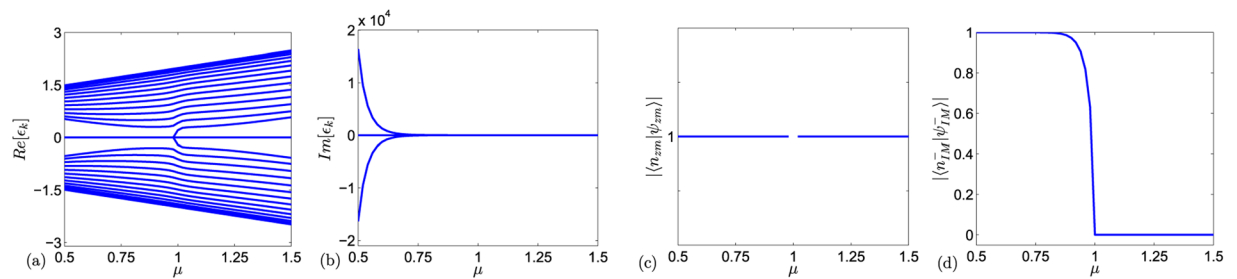


**Figure 2.** Numerical calculation of the Hamiltonian (11) when  $N=30$ . Plots (a,b) show the real part and imaginary part of eigenvalues, the zero mode exists for all  $\mu$  value and the imaginary edge mode only exists when  $\mu < 1$ . Plots (c,d) show the fidelity  $|\langle n_{zm} | \psi_{zm} \rangle|$  and  $|\langle \psi_{zm} | \psi_{zm} \rangle|$ , where  $\langle n_{zm} |$  and  $\langle \psi_{zm} |$  means the numerically calculated zero mode and one of the imaginary edge mode, respectively.

**Connection to conventional zero mode.** In this section, we investigate the connection for the zero-mode states between the present non-Hermitian model and infinite Hermitian SSH chain. We consider  $\mu_{SSH}$  in the large  $N$  limit and analyze the solutions in the following two regions.

(i) In the case of  $\mu > 1$ , we have  $\gamma = \mu^{1-N/2} \rightarrow 0$ . Matrices  $h_{SSH}$  and  $h_{SSH}^\dagger$  become the same matrix of  $N$ -site single-particle Hermitian SSH chain with open boundary conditions. Two zero-mode wave functions  $|\eta_{zm}\rangle$  and  $|\psi_{zm}\rangle$  become two degenerate zero modes of the same Hermitian SSH chain. Remarkably, the Eq. (21) for characterizing the coalescing levels is nothing but the Dirac orthogonality of two degenerate zero modes. The coalescing zero mode is the finite-size projection of the conventional degenerate zero modes in a Hermitian infinite system with the open boundary condition. In this sense, the coalescing zero modes  $|\eta_{zm}\rangle$  and  $|\psi_{zm}\rangle$  for any small  $N$  carry the complete information of conventional zero modes for the SSH chain.

(ii) Now we turn to the case of  $\mu < 1$ . In contrast to the case (i), we have  $\gamma = \mu^{1-N/2} \gg 1$ . Therefore, two ending sites are adiabatically eliminated from the  $N$ -site chain. The original system is separated into three independent parts. Two ending-site parts possess two eigenvectors with imaginary eigenvalues  $\pm i\gamma$ . The third part corresponds to an  $(N-2)$ -site single-particle Hermitian SSH chain with open boundary conditions. Although an SSH chain is at total different topological phases for  $\mu > 1$  and  $\mu < 1$  respectively. However, such an  $(N-2)$ -site Hermitian SSH chain is the same as that of the  $N$ -site one in the large  $N$  limit. In this sense, the coalescing zero mode for  $\mu < 1$  represents the same feature as that of  $\mu > 1$ .

We plot Dirac norm distribution of the coalescing zero mode from Eq. (17) for the Hamiltonian (11) with  $N=30, 22$ , and 14, where

$$P(j) = |\langle j | \psi_{zm} \rangle| = \begin{cases} \sqrt{\frac{2(1-\mu^N)}{1-\mu^2}} \mu^{N/2-l}, & j = 2l - 1, \\ \sqrt{\frac{2(1-\mu^N)}{1-\mu^2}} \mu^{l-1}, & j = 2l, \end{cases} \quad l = 1, 2, \dots, N/2, \quad (28)$$

as the demonstration of our main result (see Fig. 3). We see that systems with different size share a common part of wave vector. It indicates that one can retrieve the information of the Majorana zero mode in the thermodynamic limit from a small non-Hermitian system. Two degenerate conventional zero modes corresponds to the left and right vectors of the coalescing zero mode.

## Discussion

In conclusion, we have demonstrated a connection between the topological characterization of an infinite system and the property of a specific small system through a concrete Kitaev model. We have shown that a fine-tuned non-Hermitian  $\mathcal{PT}$ -symmetric chemical potential in the finite-size Kitaev ring results in coalescing Majorana zero mode. In particular, such a zero mode in small lattice contains all the information of the conventional degenerate Majorana zero modes in the thermodynamic limit. In addition, the number of edge modes, which includes a pair modes with imaginary eigenvalues, can be a topological invariant to characterize the quantum phase diagram of the corresponding bulk Hermitian system. Although the obtained conclusion is only based on a specific model, it may be a universal feature of the topological system. The recent studies of non-Hermitian Dirac superconductor have shown this point<sup>42,43</sup>. The underlying mechanism is two fold. Firstly, a single unit cell contains all the information about the bulk system, including the topological feature. Secondly, a finite-size non-Hermitian system, in some way, can be regarded as a sub-system embedded in an infinite system.

## Methods

**General evanescent solution for non-hermitian ssh chain.** In this section, we provide the evanescent solutions of the Hamiltonian (11) with  $\gamma < \mu^{1-N/2}$  by the Bethe ansatz method. The Bethe ansatz wave function has the form

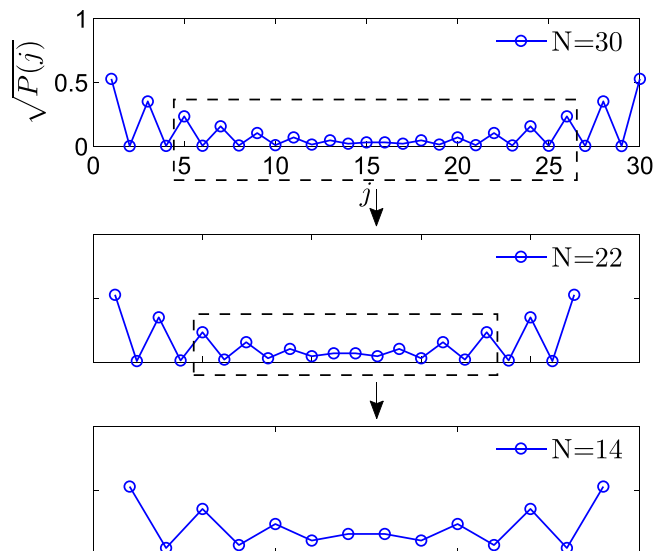


**Figure 3.** Plots of Dirac norm distribution of the coalescing zero mode from Eq. (17) for the Hamiltonian (11) with  $\mu = 1.5$   $\gamma = \mu^{1-N/2}$  for different  $N$ . The dashed boxes indicate that the plot for  $N = 22$  is a part of  $N = 30$ , while the plot of  $N = 14$  is a part of  $N = 22$ . Three systems share a common part of wave vector.

$$f_l^k = \begin{cases} A_k e^{ikl} + B_k e^{-ikl}, & l = 2j - 1 \\ C_k e^{ikl} + D_k e^{-ikl}, & l = 2j \end{cases}, \tag{29}$$

where  $j = 1, 2, \dots, N/2$ . The explicit form of Schrodinger equation

$$H|\psi_k\rangle = \varepsilon_k|\psi_k\rangle \tag{30}$$

is expressed as

$$\begin{cases} f_{m-1}^k - \mu f_{m+1}^k = \varepsilon_k f_m^k \\ f_m^k - \mu f_{m-2}^k = \varepsilon_k f_{m-1}^k \\ f_{m+2}^k - \mu f_m^k = \varepsilon_k f_{m+1}^k \\ f_{m+1}^k - \mu f_{m+3}^k = \varepsilon_k f_{m+2}^k \end{cases} \tag{31}$$

in the bulk and

$$\begin{cases} i\gamma f_1^k + f_2^k = \varepsilon_k f_1^k \\ f_{N-1}^k - i\gamma f_N^k = \varepsilon_k f_N^k \end{cases} \tag{32}$$

at two ends, where  $m = 2j, j = 1, 2, 3, \dots, N/2$ . From Eq. (31) we have the spectrum

$$\varepsilon_k = \pm \sqrt{1 + \mu^2 - \mu(e^{2ik} + e^{-2ik})}, \tag{33}$$

and coefficients

$$\frac{B_k}{D_k} = \frac{C_k}{A_k} = e^{-ik} \sqrt{\frac{1 - \mu e^{2ik}}{1 - \mu e^{-2ik}}}. \tag{34}$$

Together with Eq. (32), we get the equation about  $k$

$$\begin{aligned} & (\varepsilon_k^2 - \gamma^2 - 1)[e^{i(N-2)k} - e^{-i(N-2)k}] \\ & + \mu e^{i(N-4)k} - e^{-i(N-4)k} + \mu(\gamma^2 + \varepsilon_k^2)(e^{ikN} - e^{-ikN}) \\ & = 0. \end{aligned} \tag{35}$$

In general, the wave function  $|\psi_k\rangle$  with real  $k$  always represents the scattering vector. Since the real  $k$  is bounded by  $\pm\pi$ , the gap between two branches of eigenvalues  $\varepsilon_k$  is also bounded by  $2|1 - \mu|$ .

We are interested in the evanescent wave solution which corresponds to  $k = i\kappa$  or  $\pi + i\kappa$  ( $\kappa$  is a real number). In this case, Eq. (35) becomes

$$(\varepsilon_k^2 - \gamma^2 - 1)\sinh[(N-2)\kappa] + \mu \sinh[(N-4)\kappa] + \mu(\gamma^2 + \varepsilon_k^2)\sinh(N\kappa) = 0, \quad (36)$$

with eigenvalue

$$\varepsilon_k = \pm \sqrt{1 + \mu^2 - 2\mu \cosh(2\kappa)}. \quad (37)$$

At first, it is not hard to find that there are always two solutions

$$\kappa = \pm \frac{1}{2} \ln \mu \quad (38)$$

for Eq. (36). It leads to  $A_k = D_k = 0$  with  $\kappa = -\frac{1}{2} \ln \mu$  (or  $B_k = C_k = 0$  with  $\kappa = \frac{1}{2} \ln \mu$ ) according to Eq. (34). This solution holds for all value of  $\mu \neq 1$ . Secondly, in the case of

$$e^{-\kappa N}, e^{-\kappa(N-2)}, e^{-\kappa(N-4)} \ll 1, \quad (39)$$

Equation (36) can be reduced to

$$(\varepsilon_k^2 - \gamma^2 - 1)e^{\kappa(N-2)} + \mu e^{\kappa(N-4)} + \mu(\gamma^2 + \varepsilon_k^2)e^{\kappa N} = 0, \quad (40)$$

or a more popular form

$$e^{-4\kappa} + \frac{\varepsilon_k^2 - \gamma^2 - 1}{\mu} e^{-2\kappa} + (\gamma^2 + \varepsilon_k^2) = 0. \quad (41)$$

Submitting the expression of  $\varepsilon_k$  into the equation above, it can be approximately reduced to a linear equation for  $e^{-2\kappa}$ , which has the solution

$$\kappa = \frac{1-N}{2} \ln \mu. \quad (42)$$

We note that the relations

$$\begin{cases} \kappa_{\mu=1} = 0 \\ \frac{\partial \kappa}{\partial \mu} < 0 \end{cases} \quad (43)$$

ensure the condition in Eq. (39) can be satisfied for the region  $\mu < 1$ . Then the obtained solution is justified. A similar procedure can be performed in the case of  $e^{\kappa N}, e^{\kappa(N-2)}, e^{\kappa(N-4)} \ll 1$ . In summary, a pair of solutions with imaginary wave vectors are

$$k = \pm i \frac{1-N}{2} \ln \mu. \quad (44)$$

And the corresponding eigenvalues are

$$\varepsilon_{\text{IM}} \approx \pm i \mu^{1-N/2}. \quad (45)$$

**Example solution for  $N=6$ .** We demonstrate the above analysis via exact solutions for  $N=6$  system. Taking  $\mu=2$ , we have  $\gamma=1/4$ , matrix  $h_{\text{SSH}}$  is expressed explicitly as

$$M_1 = \begin{pmatrix} i/4 & 1 & 0 & 0 & 0 & 0 \\ 1 & 0 & 2 & 0 & 0 & 0 \\ 0 & 2 & 0 & 1 & 0 & 0 \\ 0 & 0 & 1 & 0 & 2 & 0 \\ 0 & 0 & 0 & 2 & 0 & 1 \\ 0 & 0 & 0 & 0 & 1 & -i/4 \end{pmatrix}. \quad (46)$$

The eigenvalues are



$$\begin{aligned}
 \varepsilon_1 = \varepsilon_2 &= 0, \\
 \varepsilon_3 = -\varepsilon_4 &= \frac{1}{8}\sqrt{350 + 2\sqrt{3553}}, \\
 \varepsilon_5 = -\varepsilon_6 &= \frac{1}{8}\sqrt{350 - 2\sqrt{3553}},
 \end{aligned}
 \tag{47}$$

which are all real. Two zero-mode eigen vectors are identical, i.e.,

$$\phi_1 = \phi_2 = (4i, 1, -2i, -2, i, 4), \tag{48}$$

which has zero biorthogonal norm.

Taking  $\mu = 1/2$ , we have  $\gamma = 4$ , matrix  $h_{\text{SSH}}$  is expressed explicitly as

$$M_2 = \begin{pmatrix} i4 & 1 & 0 & 0 & 0 & 0 \\ 1 & 0 & 1/2 & 0 & 0 & 0 \\ 0 & 1/2 & 0 & 1 & 0 & 0 \\ 0 & 0 & 1 & 0 & 1/2 & 0 \\ 0 & 0 & 0 & 1/2 & 0 & 1 \\ 0 & 0 & 0 & 0 & 1 & -i4 \end{pmatrix}, \tag{49}$$

The eigenvalues are

$$\begin{aligned}
 \varepsilon_1 = \varepsilon_2 &= 0, \\
 \varepsilon_3 = -\varepsilon_4 &= \frac{i}{2}\sqrt{2\sqrt{238} + 25}, \\
 \varepsilon_5 = -\varepsilon_6 &= \frac{1}{2}\sqrt{2\sqrt{238} - 25},
 \end{aligned}
 \tag{50}$$

which contains a pair of imaginary numbers. Two zero-mode eigen vectors are identical, i.e.

$$\phi_1 = \phi_2 = (i, 4, -2i, -2, 4i, 1), \tag{51}$$

which has zero biorthogonal norm. In both two cases, vectors  $\phi_1, \phi_2$  are not normalized.

**The condition of zero modes appear.** For a general situation, the Hamiltonian (11) can be rewritten as

$$\begin{aligned}
 h_{\text{SSH}} &= \sum_{l=1}^{N/2} |2l-1\rangle\langle 2l| - \sum_{l=1}^{N/2-1} \mu |2l\rangle\langle 2l+1| \\
 &+ \text{H.c.} + \mu_L |1\rangle\langle 1| + \mu_R |N\rangle\langle N|.
 \end{aligned}
 \tag{52}$$

The eigenvalue equation corresponding to this Hamiltonian can be seen as the coupled pair of equations

$$\begin{aligned}
 -\mu\phi_{2n} + \phi_{2n+2} &= E\phi_{2n+1} \\
 \phi_{2n-1} - \mu\phi_{2n+1} &= E\phi_{2n},
 \end{aligned}
 \tag{53}$$

with  $n = 1, \dots, (N/2) - 1$  together with the boundary conditions

$$\begin{aligned}
 \mu_L\phi_1 + \phi_2 &= E\phi_1, \\
 \mu_R\phi_N + \phi_{N-1} &= E\phi_N.
 \end{aligned}
 \tag{54}$$

When  $E = 0$ , it is not hard to find that

$$\begin{aligned}
 \phi_{2n+2} &= \mu\phi_{2n}, \phi_{2n+1} = \frac{1}{\mu}\phi_{2n-1}, \\
 \phi_2 &= -\mu_L\phi_1, \phi_N = -\frac{1}{\mu_R}\phi_{N-1},
 \end{aligned}
 \tag{55}$$

suppose  $\phi_1 = B, \phi_2 = A$ , the equations above give

$$\begin{aligned}
 \phi_{2n} &= A\mu^{n-1}, \phi_{2n-1} = B\frac{1}{\mu^{n-1}}, \\
 A &= -\mu_L B, A\mu^{N/2-1} = -\frac{1}{\mu_R} B\frac{1}{\mu^{N/2-1}},
 \end{aligned}
 \tag{56}$$

that means once  $E = 0$ , the two on-site potentials have to satisfy

$$\mu_L \mu_R = \frac{1}{\mu^{N-2}} \quad (57)$$

Received: 26 October 2019; Accepted: 24 March 2020;

Published online: 22 April 2020

## References

- Hasan, M. Z. & Kane, C. L. *Colloquium: Topological insulators*. *Rev. Mod. Phys.* **82**, 3045 (2010).
- Qi, X. L. & Zhang, S. C. Topological insulators and superconductors. *Rev. Mod. Phys.* **83**, 1057 (2011).
- Chiu, C. K., Teo, J. C. Y., Schnyder, A. P. & Ryu, S. Classification of topological quantum matter with symmetries. *Rev. Mod. Phys.* **88**, 035005 (2016).
- Weng, H. M., Yu, R., Hu, X., Dai, X. & Fang, Z. Quantum anomalous Hall effect and related topological electronic states. *Adv. Phys.* **64**, 227 (2015).
- Asboth, J. K., Oroszlány, L. & Pályi, A. *A short course on topological insulators: Band-structure topology and edge states in one and two dimensions* (Springer, 2016).
- Pikulina, D. I. & Nazarov, Y. V. Topological properties of superconducting junctions. *JETP Letters*. **94**, 693–697 (2011).
- Avila, J., Peñaranda, F., Prada, E., San-Jose, P. & Aguado, R. Non-hermitian topology as a unifying framework for the Andreev versus Majorana states controversy. *Commun. Phys.* **2**, 133 (2019).
- Kawabata, K., Shiozaki, K., Ueda, M. & Sato, M. Symmetry and Topology in Non-Hermitian Physics. *Phys. Rev. X* **9**, 041015 (2019).
- Jin, L. & Song, Z. Physics counterpart of the *PT* non-Hermitian tight-binding chain. *Phys. Rev. A* **81**, 032109 (2010).
- Jin, L. & Song, Z. Partitioning technique for discrete quantum systems. *Phys. Rev. A* **83**, 062118 (2011).
- Jin, L. & Song, Z. A physical interpretation for the non-Hermitian Hamiltonian. *J. Phys. A: Math. Theor.* **44**, 375304 (2011).
- Kitaev, A. Y. Unpaired Majorana fermions in quantum wires. *Physics-Uspekhi* **44**, 131 (2001).
- Mourik, V. *et al.* Signatures of Majorana Fermions in Hybrid Superconductor-Semiconductor Nanowire Devices. *Science* **336**, 1003–1007 (2012).
- Rokhinson, L. P., Liu, X. & Furdyna, J. K. The fractional a.c. Josephson effect in a semiconductor–superconductor nanowire as a signature of Majorana particles. *Nat. Phys.* **8**, 795–799 (2012).
- Das, A. *et al.* Zero-bias peaks and splitting in an Al–InAs nanowire topological superconductor as a signature of Majorana fermions. *Nat. Phys.* **8**, 887–895 (2012).
- Finck, A. D. K., Harlingen, D. J. V., Mohseni, P. K., Jung, K. & Li, X. Anomalous Modulation of a Zero-Bias Peak in a Hybrid Nanowire-Superconductor Device. *Phys. Rev. Lett.* **110**, 126406 (2013).
- Banerjee, A. *et al.* Proximate Kitaev quantum spin liquid behaviour in a honeycomb magnet. *Nature Materials*. **15**, 733–740 (2016).
- San-Jose, P., Cayao, J., Prada, E. & Aguado, R. Majorana bound states from exceptional points in non-topological superconductors. *Sci. Rep.* **6**, 21427 (2016).
- Albrecht, S. M. *et al.* Exponential protection of zero modes in Majorana islands. *Nature* **531**, 206–209 (2016).
- Deng, M. T. *et al.* Majorana bound state in a coupled quantum-dot hybrid-nanowire system. *Science* **354**, 1557–1562 (2016).
- Lutchyn, R. M. *et al.* Majorana zero modes in superconductor–semiconductor heterostructures. *Nat. Rev. Mater.* **3**, 52–68 (2018).
- Guo, A. *et al.* Observation of *PT*-Symmetry Breaking in Complex Optical Potentials. *Phys. Rev. Lett.* **103**, 093902 (2009).
- Peng, B. *et al.* Parity–time-symmetric whispering-gallery microcavities. *Nat. Phys.* **10**, 394–398 (2014).
- Hodaiei, H., Miri, M. A., Heinrich, M., Christodoulides, D. N. & Khajavikhan, M. Parity-time-symmetric microring lasers. *Science* **346**, 975–978 (2014).
- Lee, T. E. & Chan, C. K. Heralded Magnetism in Non-Hermitian Atomic Systems. *Phys. Rev. X* **4**, 041001 (2014).
- Ashida, Y., Furukawa, S. & Ueda, M. Parity-time-symmetric quantum critical phenomena. *Nat. Commun.* **8**, 15791 (2017).
- Kawabata, K., Ashida, Y., Katsura, H. & Ueda, M. Parity-time-symmetric topological superconductor. *Phys. Rev. B* **98**, 085116 (2018).
- Li, C., Lin, S., Zhang, G. & Song, Z. Topological nodal points in two coupled Su-Schrieffer-Heeger chains. *Phys. Rev. B* **96**, 125418 (2018).
- Lin, S., Zhang, G., Li, C. & Song, Z. Magnetic-flux-driven topological quantum phase transition and manipulation of perfect edge states in graphene tube. *Sci. Rep.* **6**, 31953 (2016).
- Zhang, G., Li, C. & Song, Z. Majorana charges, winding numbers and Chern numbers in quantum Ising models. *Sci. Rep.* **7**, 8176 (2017).
- Lin, S., Zhang, X. Z., Li, C. & Song, Z. Long-range entangled zero-mode state in a non-Hermitian lattice. *Phys. Rev. A* **94**, 042133 (2016).
- Klett, M., Cartarius, H., Dast, D., Main, J. & Wunner, G. Relation between *PT*-symmetry breaking and topologically nontrivial phases in the Su-Schrieffer-Heeger and Kitaev models. *Phys. Rev. A* **95**, 053626 (2017).
- Mostafazadeh, A. Pseudo-Hermiticity versus *PT* symmetry: The necessary condition for the reality of the spectrum of a non-Hermitian Hamiltonian. *J. Math. Phys.* **43**, 205 (2002).
- Jin, L. & Song, Z. Solutions of *PT*-symmetric tight-binding chain and its equivalent Hermitian counterpart. *Phys. Rev. A* **80**, 052107 (2009).
- Schomerus, H. Topologically protected midgap states in complex photonic lattices. *Opt. Lett.* **38**, 1912–1914 (2013).
- Poli, C., Bellec, M., Kuhl, U., Mortessagne, F. & Schomerus, H. Selective enhancement of topologically induced interface states in a dielectric resonator chain. *Nat. Commun.* **6**, 6710 (2015).
- Zeuner, J. M. *et al.* Observation of a Topological Transition in the Bulk of a Non-Hermitian System. *Phys. Rev. Lett.* **115**, 040402 (2015).
- Weimann, S. *et al.* Topologically protected bound states in photonic parity-time-symmetric crystals. *Nat. Mater.* **16**, 433–438 (2017).
- Zeng, Q. B., Zhu, B. G., Chen, S., You, L. & Lü, R. Non-Hermitian Kitaev chain with complex on-site potentials. *Phys. Rev. A* **94**, 022119 (2016).
- Menke, H. & Hirschmann, M. M. Topological quantum wires with balanced gain and loss. *Phys. Rev. B* **95**, 174506 (2017).
- Liu, X. J., Wong, C. L. M. & Law, K. T. Non-Abelian Majorana Doublets in Time-Reversal-Invariant Topological Superconductors. *Phys. Rev. X* **4**, 021018 (2014).
- Zyuzin, A. A. & Simon, P. Disorder-induced exceptional points and nodal lines in Dirac superconductors. *Phys. Rev. B* **99**, 165145 (2019).
- Ge, Z. Y. *et al.* Topological band theory for non-Hermitian systems from the Dirac equation. *Phys. Rev. B* **100**, 054105 (2019).

## Acknowledgements

We acknowledge the support of the CNSF (Grant No. 11874225).

### Author contributions

C.L., L.J. & Z.S. did the derivations and edited the manuscript. Z.S. conceived the project and drafted the manuscript. All authors reviewed the manuscript.

### Competing interests

The authors declare no competing interests.

### Additional information

**Correspondence** and requests for materials should be addressed to Z.S.

**Reprints and permissions information** is available at [www.nature.com/reprints](http://www.nature.com/reprints).

**Publisher's note** Springer Nature remains neutral with regard to jurisdictional claims in published maps and institutional affiliations.



**Open Access** This article is licensed under a Creative Commons Attribution 4.0 International License, which permits use, sharing, adaptation, distribution and reproduction in any medium or format, as long as you give appropriate credit to the original author(s) and the source, provide a link to the Creative Commons license, and indicate if changes were made. The images or other third party material in this article are included in the article's Creative Commons license, unless indicated otherwise in a credit line to the material. If material is not included in the article's Creative Commons license and your intended use is not permitted by statutory regulation or exceeds the permitted use, you will need to obtain permission directly from the copyright holder. To view a copy of this license, visit <http://creativecommons.org/licenses/by/4.0/>.

© The Author(s) 2020